LITERATURE CITED

1. L. Sigerlind, Use of the Finite Element Method [Russian translation], Mir, Moscow (1979).
2. J. Conner and K. Brebbia, Finite Element Method in Fluid Mechanics [Russian translation], Sudostroenie, Leningrad (1979).
3. O. Zenkevich, Finite Element Method in Engineering [Russian translation], Mir, Moscow (1975).
4. Yu. P. Vorob'ev, N. V. Zezyulya, V. U. Lemeshev, et al., "Effectiveness of finning in a chemically reactive heat carrier," in: Dissociating Gases as Heat Carriers and Working Substances in Power Plants [in Russian], Part 2, ITMO, Minsk (1973), pp. 194-202.
5. A. A. Samarskii, Introduction to the Theory of Difference Methods [in Russian], Nauka, Moscow (1971).
6. B. S. Petukhov, L. G. Genin, and S. A. Kovalev, Heat Exchange in Nuclear Power Plants [in Russian], Atomizdat, Moscow (1974).
7. V. E. Minashin, A. A. Sholokhov, and Yu. I. Gribanov, Thermophysics of Nuclear Reactors with Liquid-Metal Cooling and Methods of Electrical Modeling [in Russian], Atomizdat, Moscow (1971).
8. V. A. Nemtsev and V. I. Nikolaev, "Study of hydrodynamics and heat exchange in laminar flow about tubes with longitudinal fins by the method of electrohydrodynamic analogy," Izv. Akad. Nauk BSSR, Ser. FEN, No. 1, 79-83 (1982).
9. Ma-Tin-Ji, Development of Heat Transfer in Tubes with Laminar Flow [Russian translation], Izv. Akad. Nauk SSSR, Moscow (1962), pp. 27-42.

PHYSICAL FEATURES OF THE EVAPORATIVE LIQUID COOLING OF A POROUS METAL—CERAMIC FUEL ELEMENT

V. A. Maiorov and L. L. Vasil'ev

UDC 536.24:532.685

This article compares calculated data with results of an experimental study of the temperature field of a porous metal—ceramic fuel element during its evaporative liquid cooling and reports physical features of this process.

The study [1] showed analytically that the evaporation of a liquid flow inside a porous heated metal is characterized by a limiting high rate of heat transfer. The literature presently does not have the empirical data needed to back up this theoretical finding. For example, the small thickness of the porous plates used in the well-known study [2] does not provide an evaporation region inside the porous metal in the two-phase-flow discharge regime which is long enough to measure temperature, and there is no possibility of stable operation in the regime of superheated-vapor discharge.

Presented below is empirical data on the cooling of porous stainless-steel specimens in the form of rectangular bars 10 × 16 × 125 mm by distilled water. The bars are heated by a direct electrical current. The study [3] described the specimens and the results of investigation of the structure of the outgoing two-phase flow and the temperature field on the outer surface. The temperature through the specimen thickness was measured at two stations along the bar. Here, thermocouples were embedded into channels drilled along a normal to the lateral surface on one side. These channels were drilled to the middle of the bar. The distorting effect of the channels on the flow of coolant and the temperature field was reduced by displacing them alternately 2-3 mm heightwise in the direction of the cross section of interest. With a constant coolant discharge, we gradually increased the power supplied to the specimen. We began with the regime of discharge of a subheated (relative to boiling)

Novolipetsk Polytechnic Institute. A. V. Lykov ITMO, Academy of Sciences of the Belorussian SSR. Translated from Inzhenerno-Fizicheskii Zhurnal, Vol. 46, No. 2, pp. 189-195, February, 1984. Original article submitted November 3, 1982.

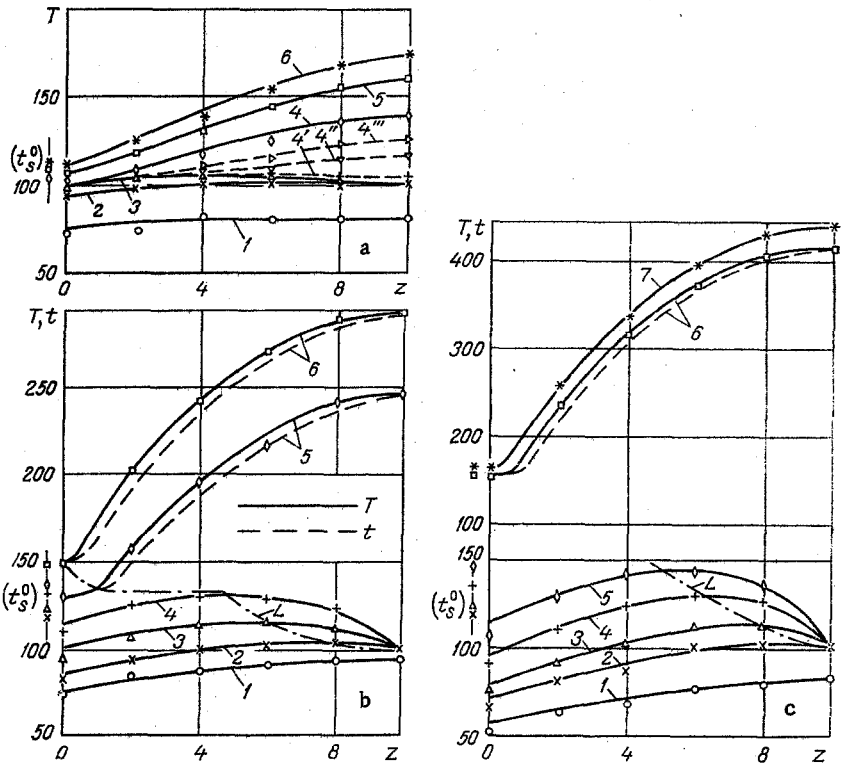

Fig. 1. Change in the thermal state of the porous fuel element with different mass discharges of the coolant: a) G = 0.040 kg/m²•sec (sequential increase in volumetric heat release), specimen No. 18; b) 0.158, specimen No. 20; c) 0.332, specimen No. 20 (explanations in Table 1). T, t, °C; Z, mm.

TABLE 1. Experimental and Theoretical Parameters in Fig. 1

Exptl. parameters			Theor. parameters							
designation	$q_v \cdot 10^{-7}$, W/m²	t_s^0, °C	$B=\frac{G\delta c'}{\lambda}$	$A=\frac{}{h_v\delta/Gc'}$	l	$t_s(L)$, °C	$k-l$	k	E_1	E_3
Fig. 1a, specimen № 18, $G = 0{,}040$ kg/m²•sec										
1	0,56	102	0,14	26	—	—	—	—	—	—
2	0,86	102	0,14	26	0,50	101	—	—	1,00	—
3	1,49	102	0,14	26	0,25	102	—	—	1,00	—
4′	1,62	102	4′ — 4″ — 4‴ — intermediate states after 48 sec in the transitional regime of drying of the outer surface							
4″	1,62	103								
4‴	1,62	104								
4	1,62	105	0,132	26	0,13	104	0,02	0,15	1,00	30,0
5	1,94	108	0,126	26	0,04	107	0,02	0,06	0,30	22,9
6	2,17	112	0,140	26	0,00	111	0,03	0,03	0,00	20,0
Fig. 1b										
1	0,73	116	0,530	26	—	—	—	—	—	—
2	1,16	121	0,530	26	0,80	105	—	—	1,00	—
3	2,24	124	0,530	26	0,60	116	—	—	1,00	—
4	3,67	135	0,530	26	0,50	130	—	—	1,00	—
5	3,95	137	0,486	26	0,09	134	0,03	0,12	0,55	10,7
6	5,00	148	0,525	26	0,00	148	0,03	0,03	0,00	9,5
Fig. 1c										
1	1,20	119	1,11	26	—	—	—	—	—	—
2	1,73	119	1,11	26	0,90	102	—	—	1,00	—
3	3,00	124	1,11	26	0,80	113	—	—	1,00	—
4	4,64	135	1,11	26	0,65	130	—	—	1,00	—
5	7,80	148	1,11	26	0,50	143	—	—	1,00	—
6	8,05	160	1,04	26	0,05	158	0,03	0,08	0,28	5,5
7	8,90	165	1,01	26	0,00	165	0,04	0,04	0,00	5,5

TABLE 2. Parameters of the Process in Regimes of Discharge of a Two-Phase Flow with Maximum Depth of the Beginning of the Evaporation Region

Specimen	$q_v \cdot 10^{-7}$, W/m³	t_s^0, °C	T^*_{max}, °C
	$G = 0{,}158$ kg/m²·sec		
18	3,3	120	119
20	2,94	128	122
	$G = 0{,}332$ kg/m²·sec		
21	6,6	111	107
20	6,6	144	140
	$G = 0{,}65$ kg/m²·sec		
21	13,9	123	117
20	11,8	163	158

liquid from the specimen and ended with the regime in which the liquid begins to boil on the inside surface of the specimen. The mean volumetric heat release q_v was calculated from the power supplied to the specimen. We covered a range $q_v = (0.5\text{-}14) \cdot 10^7$ W/m³ in the tests. The unit mass discharge of water ranged from 0.04 to 0.65 kg/m²·sec.

Figure 1a-c shows some of the resulting test data on the temperature distribution of the porous element through its thickness. The parameters of the corresponding regimes are shown in Table 1. The results in each figure correspond to a series of measurements with a constant mass discharge of coolant and a sequential increase in the volumetric heat release (heat flux). The coordinate Z was directed from the inside surface. Values t_s^0 of the saturation temperature at the pressure ahead of the specimen are indicated by the corresponding symbols to the left of the y axis.

The same figures show results of calculations by the method described in [1]. The solid curves denote theoretical distributions of the temperature T of the porous material, while the dashed curves denote the temperature of the coolant. The values of the parameters used in the calculations are shown in Table 1. They were determined from characteristics of the specimens and regime parameters.

Curves 1 in Fig. 1 correspond to the regime of single-phase cooling without boiling of the water. Here, the temperature of the coolant differs only slightly (by 1-2°C) from the temperature of the porous material. The good agreement between the test and calculated data is evident, as is the tendency for the slope of curve 1 to increase as coolant discharge increases.

Of considerable interest are the temperature profiles in the regimes of discharge of an evaporating two-phase flow — 2-3 in Fig. 1a, 2-4 in Fig. 1b, and 2-5 in Fig. 1c. A distinguishing feature of these profiles is the fixed temperature of 100°C on the outer surface and the presence of a maximum inside the specimen. These temperature profiles for the porous metal have the following sections: an initial section of an increase in temperature with single-phase liquid flow of the coolant; a maximum corresponding to the beginning of the evaporation region; an outlet section corresponding to a drop in temperature with the presence of a two-phase evaporating flow, the temperature of the vapor phase here being equal to the local saturation temperature t_s and decreasing due to the pressure drop in the flow.

An increase in the volumetric heat release is accompanied by a shift in the temperature maximum to the inside surface of the specimen — the data for each in Fig. 1a-c. The mass vapor content in the outgoing two-phase flow increases. The study [3] also reported observing a change in the pattern of discharge of the evaporating two-phase flow on the outer surface. The temperature maximum increases in the changeover to a series of experiments with a higher coolant discharge. The dot—dash lines L in Fig. 1b and c represent the dependence of the temperature of the porous material at the beginning of the evaporation region on its coordinate Z = L and they pass through the maximum of the temperature profiles.

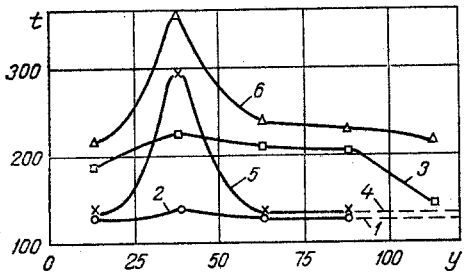

Fig. 2

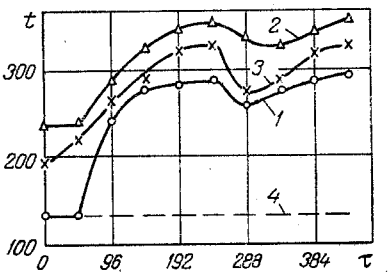

Fig. 3

Fig. 2. Temperature distribution along the inner and outer surfaces of the element before and after formation of the vapor layer on part of the inside surface: 1) saturation temperature t_s^0 at the pressure ahead of the inlet to the specimen; 2, 3) temperatures of the inner and outer surfaces before the formation of the vapor layer; 4-6) same respective quantities after formation of the vapor layer. Specimen No. 20, $q_v = 3.16 \cdot 10^7$ W/m^3, G = 0.082 kg/m^2·sec. y, mm.

Fig. 3. Change in temperature with time at certain points through the thickness of the element in a section of local overheating with the formation of the vapor layer: 1, 2) temperature of the inside and outside surfaces; 3) at a distance of 4 mm from the specimen inlet; 4) saturation temperature t_s^0. Specimen No. 20, $q_v = 3.16 \cdot 10^7$ W/m^3, G = 0.082 kg/m^2·sec. τ, sec.

The maximum temperature T_{max} of the porous material inside the specimen is affected mainly by the local saturation temperature $t_s(L)$ at the beginning of the evaporation zone. The volumetric heat release q_v has a slight effect on T_{max}. This can be seen from the data in Table 2, which compares results for specimens with different hydraulic characteristics (different values of the pressure drop on the specimen and different saturation temperatures t_s^0 before the specimen) with the same mass discharges of coolant and roughly the same volumetric heat releases q_v. Here T_{max}^* is the temperature of the porous material corresponding to the maximum with maximum penetration (depth) of the front of the evaporation zone in the last regime before the beginning of drying of the outer surface, i.e., the maximum temperature with a fixed discharge. Since it is always the case that $T_{max}^* < t_s^0$, we can conclude that T_{max}^* negligibly exceeds the value $t_s(L)$, i.e., the coolant begins to boil in the porous metal without appreciable superheating. It should be noted that $t_s(L) < t_s^0$ due to the pressure drop on the liquid section. The magnitude of this drop was not determined due to an uncontrolled increase in the resistance of the inlet section resulting from its obstruction by mechanical impurities from the paronite side gaskets.

The continuous decrease in the temperature of the porous material with a decrease in the saturation temperature of the vapor phase of the evaporating two-phase flow and the absence of appreciable overheating of the porous material ($T - t_s \lesssim 1°C$) at the beginning of the evaporation zone and on the outer surface with levels of heat release corresponding to discharge of the evaporating flow up to $q_v = 1.18 \cdot 10^8$ W/m^3 are evidence of the fact that the rate of volumetric heat transfer during evaporation of the flow inside the porous material is very high: $h_v \approx q_v/(T - t_s) \approx 1.2 \cdot 10^8$ W/(m^3·°K). This is in agreement with the qualitative estimates made in [1].

With a further increase in heat flux after the regimes with discharge of the two-phase mixture there follow regimes with gradual drying of the outer surface. The character of its drying depends on the level of the heat flux and the uniformity of the structure of the specimen.

With a volumetric heat release $q_v < 2.5 \cdot 10^7$ W/m^3, a substantial part of the specimen surface dries. Curves 4'–4''–4''' in Fig. 1a show nonstationary intermediate temperature fields typical of the beginning of the drying of the outer surface. The change in temperature occurs fairly slowly. The steady state is represented by curve 4.

With $q_v = (2.5\text{-}8.0) \cdot 10^7$ W/m^3, usually a relatively short length of the outer surface dries first. The drying of the rest of the surface is drawn out by the redistribution of the coolant flow and heat flux along the specimen. Due to an increase in hydraulic resistance, coolant discharge decreases on the dried parts of the surface and increases on the sections

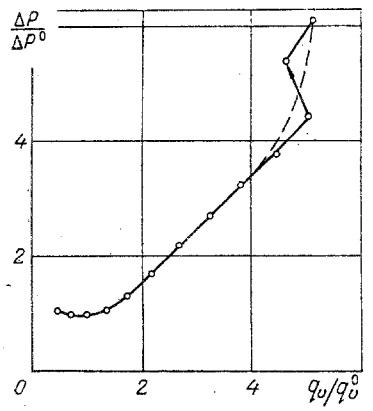

Fig. 4. Dependence of the pressure drop on the porous fuel element on the heat flux. Specimen No. 20, G = 0.332 kg/m²•sec, q_v^0 = $1.73 \cdot 10^7$ W/m³, ΔP^0 = 0.1 MPa.

covered by a boiling film. With a constant density j of the electrical current over the specimen cross section, the heat flux $q_v = j^2\rho$ increases with an increase in the electrical resistance ρ in the dry zone due to an increase in the temperature of the porous material. At such levels of heat flux there is a jump in the values of the parameters (such as the temperature of the outer surface and the coordinate L of the beginning of the evaporation region) in the transition from the regime of discharge of a two-phase flow to the regime of complete evaporation of the flow inside the porous material along the entire length of the specimen. Figure 1b shows the corresponding temperature distributions in the steady state.

In forced cooling regimes with a heat flux $q_v > 8 \cdot 10^7$ W/m³ at the moment of appearance of dry spots on the surface, the dry zone quickly spreads over the entire specimen surface. It is interesting to note here that maintaining a constant voltage on the specimen in such a regime leads to a marked decrease in the mean heat flux due to an increase in the electrical resistance of the porous metal with an increase in its temperature. Figure 1c, curve 6, shows the temperature distribution through the specimen thickness after drying of its entire outer surface.

Comparison of the theoretical and experimental data on the temperature distribution shows that they agree well over the entire specimen height. In the regimes of discharge of superheated vapor, heat transfer in the evaporation region and the length of this region were calculated for the mean rate of volumetric heat release $h_v = 3 \cdot 10^8$ W/(m³•K). The agreement between the theoretical and empirical data on temperature distribution in the vapor section of coolant flow shows that the test data on the length of the evaporation zone does not exceed the theoretical data. Thus, the rate of volumetric heat release in it is high (at least no lower than $h_v = 3 \cdot 10^8$ W/(m³•K)) and, with $q_v = 1.4 \cdot 10^8$ W/m³, the relative extent of this zone is small ($k - \zeta < 0.03$). Thus, it may with sufficient accuracy be considered the surface.

The temperature difference T − t between the porous metal and the coolant is maximal at the beginning of the vapor section and gradually decreases toward the outer surface (Fig. 1b, c). This quantity does not exceed 16°C at the beginning of the vapor section and does not exceed 1.5°C at the outlet of the element in the most forced regimes.

The substantial increase in the temperature of the outer surface attendant to its complete drying and the abrupt shortening of the evaporation zone are accompanied by advance of the evaporation front into the specimen and an increase in the temperature of its inside surface. A further increase in volumetric heat release causes the front to move deeper into the specimen, and it eventually reaches the inside surface. The temperature of this surface becomes equal to the saturation temperature t_s^0 at the given pressure ahead of the specimen. This situation is reflected by curves 6 in Fig. 1a and b and curve 7 in Fig. 1c.

Finally, the liquid on the upturned horizontal inlet surface begins to boil. This is accompanied by the formation of a vapor layer and a sharp increase in the temperature of the inside surface. The vapor layer is formed not on the entire inside surface but rather only on part of it (this follows from the data in Fig. 2). It is quite evident that the overheating is distinctly local in character and penetrates deeper as a result of redistribution of the flow of coolant and the heat flux along the specimen: flow rate decreases in the overheated region and heat flux increases.

Figure 3 shows the change in temperature at certain points over the specimen height in the overheated section with the formation of a vapor layer ahead of the specimen inlet. It follows from this that after it forms, the vapor layer on the inlet surface subsequently remains stable. The length and position of the overheated region are determined by the characteristics of the specimen.

With a fixed coolant flow rate and an increase in the volumetric heat release, the pressure drop on the porous element increases as a result of an increase in the mass vapor content of the outgoing flow. Figure 4 shows data typical of such a situation. The fixed values of the pressure drop on the specimen ΔP° and the volumetric heat release q_v° pertain to the regime in which the liquid begins to boil on the outer surface of the element.

One feature of the dependences in Fig. 4 is the minimum corresponding to the beginning of boiling on the outer surface. In the regimes of single-phase liquid cooling ($q_v/q_v^{\circ} < 1$), as heat flux increases so does the mean temperature of the coolant inside the porous material, which in turn causes a decrease in its viscosity and the pressure drop. As the coolant begins to boil inside the porous element ($q_v/q_v^{\circ} > 1$), an increase in the depth of the evaporation front and the vapor content of the flow leads to a nearly linear increase in the pressure drop. Then, in a new regime, a substantial portion of the outer surface quickly dries and the pressure drop increases sharply. The increase in the mean temperature of the porous metal causes a substantial increase in its electrical resistance, which with a constant voltage on the specimen leads to a decrease in the mean volumetric heat release. The change in the parameters in this regime is shown by the arrow pointing upward to the left and located between two points corresponding to the beginning and end of this regime. A subsequent increase in the heat release is accompanied by drying of the entire surface, and the latter point corresponds to the regime of discharge of superheated vapor with a completely dry outer surface. The dashed line represents the change in the parameters with uniform drying of the outer surface and a gradual increase in its temperature — a situation which prevails in the case of moderate thermal loads.

In conclusion, we should note that the above experiments resulted in stable, long-term operation of the system investigated, including in regimes with the discharge of superheated steam at a temperature of 500°C or more. This was achieved by arranging for a constant coolant discharge and using porous specimens of considerable thickness.

LITERATURE CITED

1. V. A. Maiorov and L. L. Vasil'ev, "Heat transfer in the region of evaporation of a coolant inside a porous fuel element," Inzh.-Fiz. Zh., 46, No. 1, 8-14 (1984).
2. V. M. Polyaev and A. V. Sukhov, "Physical features of heat transfer in the flow of a liquid with phase transformations through a porous wall," Teplofiz. Vys. Temp., 7, No. 5, 1037-1039 (1969).
3. V. A. Maiorov and L. L. Vasil'ev, "Structure of an evaporating flow inside heated porous metal," Inzh.-Fiz. Zh., 41, No. 6, 965-969 (1981).